Supporting Information

Giant Auxetic Behavior in Remote-plasma Synthesized Few-Layer Tungsten Semicarbide

Noah B. Stocek[1], Farman Ullah[1,*], and Giovanni Fanchini[1,2,**]

[1]*Department of Physics and Astronomy, The University of Western Ontario, 1151 Richmond St. London, ON, N6A 3K7, Canada*

[2]*Department of Chemistry, The University of Western Ontario, 1151 Richmond St. London, ON, N6A 5B7, Canada*

Table of contents

S1. Model of ion selectiveness in remote plasmas extracted by DC voltages

Here we present a model elucidating the dynamics of ions being extracted from the plasma chamber of the remote plasma physical vapor deposition chamber used in this work. The DC-voltage applied between the plasma chamber and the deposition tube extracts the discharge into the tube, however this extraction is impeded by the backflowing Ar that is introduced from the far side of the tube. Crucially, there is a certain range of values of Ar backflow magnitude which allows for only extraction of the heavier W_2C ions, while lighter WC ions are rejected via Ar atom collisions. Figure S.1 shows the two scenarios of ion extraction, where low Ar backflow (Fig S.1a) allows all ions to be extracted from the plasma and into the deposition tube, while higher backflow (Fig S.1b) allows for only heavier ions, such as W_2C to be extracted.

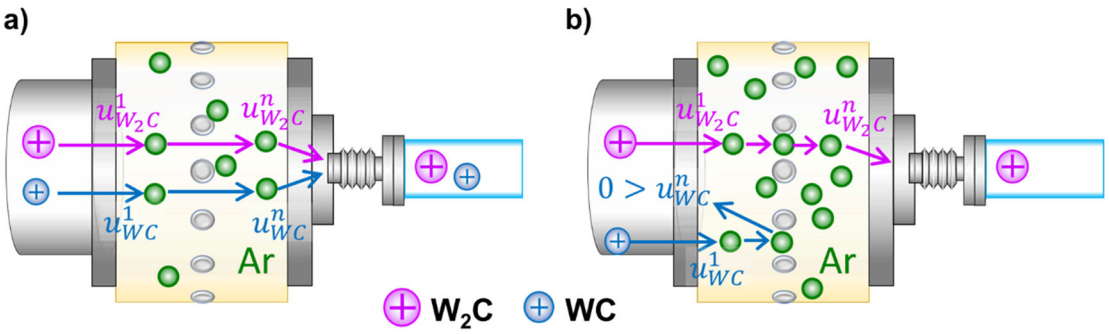

Figure S1. Collisions between extracted ions and backflowing Ar atoms for a) low Ar backflow and b) high Ar backflow. For low backflow, the Ar density is low enough that all ions gain more energy between collisions than they lose during collisions. For higher Ar density, collisions are more frequent and therefore less energy is gained; for lighter ions, this is less than the energy lost during collisions, and extraction from the plasma is prevented.

As ions diffuse from the plasma chamber into the extraction flange, they experience positive acceleration (towards the substrate) due to the electric field, and negative acceleration due to

collisions with backflowing Ar atoms. The distance between these collisions is L_p, which depends on the magnitude of the Ar backflow, and for our experiments was on the order of 30 mm for no Ar backflow and decreased to 20 mm for 5 sccm of Ar backflow. The energy gained over this distance is eL_pV_0/L_0, where V_0 is the applied voltage of -2000 V and L_0 is the thickness of the flange of 1 inch. Thus, if the velocity of the ion immediately after the nth collision is $v_i^{(n)}$, then the velocity immediately before the n+1 collision is

$$u_i^{(n+1)} = \sqrt{v_i^{(n)2} + \frac{2eL_pV_0}{m_iL_0}}. \qquad (S.1.1)$$

The velocity of the backflowing Ar atoms is determined by their thermal velocity as they diffuse towards the plasma chamber and is

$$v_{Ar} = \sqrt{\frac{2k_BT}{m_{Ar}}}. \qquad (S.1.2)$$

Considering an inelastic collision between the forward flowing ions, and the backflowing Ar atoms, the velocity immediately after the n=1 collision is

$$v_i^{(n+1)} = \frac{m_i}{m_i + m_{Ar}}\left(\sqrt{v_i^{(n)2} + \frac{2eL_pV_0}{m_iL_0}}\right) - \frac{m_{Ar}}{m_i + m_{Ar}}\sqrt{\frac{2k_BT}{m_{Ar}}}. \qquad (S.1.3)$$

The first term in this equation would be the post-collision velocity for stationary Ar atoms, and the second term contains a backwards component from the argon's velocity.

Equation (S.1.3) allows us to analyze the acceleration of ions being extracted in the flange, and to compare their velocities as they enter the tube, which is crucial for determining which ions reach the substrate. The first term in equation (S.1.3) depends on both the ion mass, as the factor in front approaches unity for high ion mass, and on the Ar backflow, as higher flow leads to lower L_p, and less time to accelerate between collisions. This term is at its highest for heavier ions and

low backflow and decreases for lower ion mass and/or higher backflow. The second term only depends inversely on the ion mass, as it approaches 0 for heavier ions. This means that lighter ions are more sensitive to the backwards "kick" from flowing Ar, and less likely to retain positive velocity.

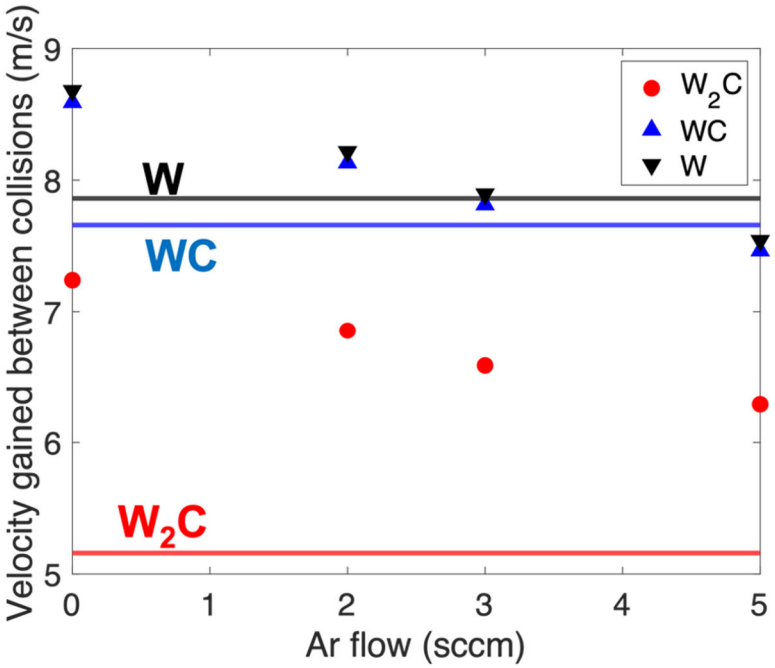

Figure S2. Comparison of the velocity gained between collisions for relevant ions (which varies with Ar flow) and the velocity lost for each collision (which depends only on ion mass). Velocity gained is shown as dots, and the constant value of velocity lost is shown by solid lines. When velocity gained is lower than velocity lost, which occurs with W and WC for 5 sccm Ar backflow, the ions are not extracted through the flange.

Using equation (S.1.3) to analyze the motion of $W_2CH_n^+$, WCH_n+, and W^+ ions for the Ar pressures recorded in this experiment, the decrease L_p for higher Ar flow drops sufficiently, that for lighter ions with a lower value of $m_i/(m_i + m_{Ar})$, the forward contribution in (S.1.1) becomes smaller than the negative second term. In this case, over one acceleration-collision sequence, the final

velocity is negative. However, for the larger W_2C ions, $m_i/(m_i + m_{Ar})$ is sufficiently large (0.93 compared to 0.83 for WC) and $m_i/(m_i + m_{Ar})$ is sufficiently small that the positive term remains larger, and after each acceleration-collision sequence the net velocity is positive, and continues to increase slightly after each successive sequence. Comparison of these velocity contributions are shown in Figure S2, where for 5 sccm of Ar backflow, the positive contribution (dots) becomes smaller than the negative contribution (solid lines) for WC and W. So, despite the heavier ions accelerating less between collisions, they lose less energy per collision, and there exists a window of values of Ar backflow that allow just these heavier ions to be extracted and deposited.

S2. Optimization of temperature and methane concentration in the deposition conditions

The growth conditions presented in the paper result from the preliminary optimization of two other parameters: substrate temperature in the furnace, and argon-to-methane ratio in the plasma, as demonstrated by optical microscope images in Figure S2, which are representative of deposits on top of their Cu substrate (bottom) as well as a bare substrate annealed in Ar (in the absence of plasma and carbonaceous precursors) inside the same furnace.

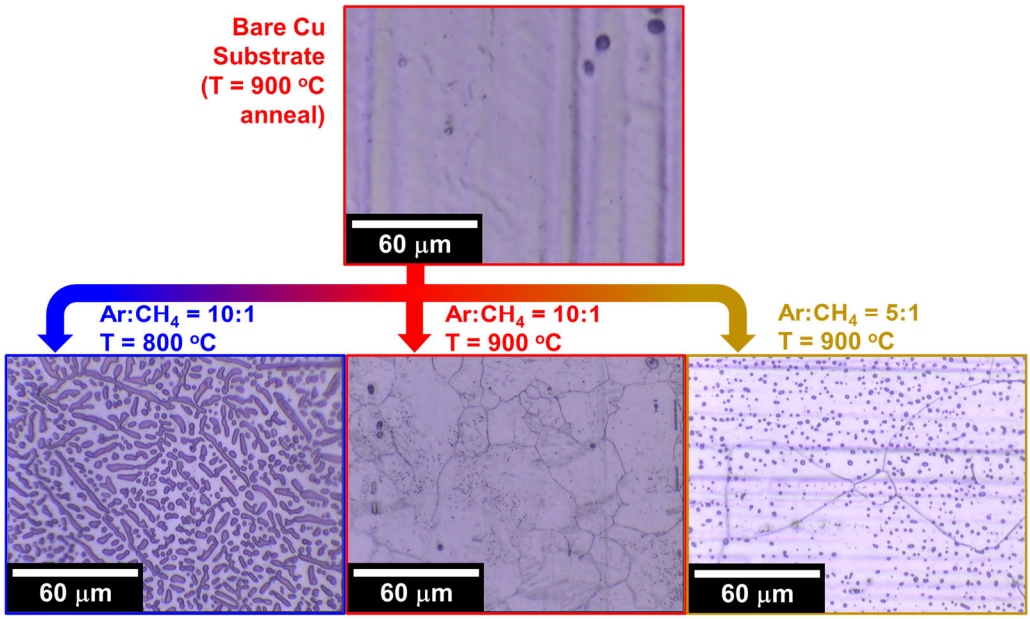

Figure S3 – Optical microscope images demonstrating the optimization of the furnace temperature and Ar:CH_4 concentration in the deposition process for FL-W_2C. It can be observed that, at 800°C, segregation of tungsten from an amorphous carbonaceous phase occurs (left), where, at 900°C (center) the same conditions yield substrate coverage by a homogeneous material, with cracks indicating boundaries among neighboring growth domains when growth is prolonged for a sufficiently long time. If the Ar:CH_4 ratio is increased to 5:1 (right) graphitic microparticles tend to seed inside the tungsten carbide domains observed at 10:1 Ar:CH_4 ratio, thus indicating an excess of carbon precursor. All of the three images (bottom) are markedly different from the bare Cu substrate.

S3. Comparison of two-dimensional W_2C with other auxetic materials

Year	-ν	Material
2014	-0.059	FL-Phosphorene
2015	-0.037	Boron Phosphide
2015	-0.08	Penta-graphene
2015	-0.02	Penta-BN2
2016	-0.1	Graphene
2016	-0.027	SL-Phosphorene
2017	-0.267	delta-Phosphorene
2017	-0.055	Tetra-silicene
2017	-0.15	SL-Mo2C
2018	-0.4	SL-W2C
2018	-0.09	alpha-Arsenene
2018	-0.042	SiC6
2019	-0.022	SL-PdSe2